DOI: 10.1002/cmdc.200800209

Nanostructure Formation Enhances the Activity of LPS-Neutralizing Peptides

Carlos Mas-Moruno,[a, b] Laura Cascales,[c] Luis J. Cruz,[a, b] Puig Mora,[c] Enrique Pérez-Payá,[c, d] and Fernando Albericio*[a, b, e]

Peptides that interact with lipopolysaccharide (LPS) can provide the basis for the development of new antisepsis agents. In this work, several LPS-neutralizing acyl peptides derived from LALF, BPI, and SAP were prepared, structurally characterized, and biologically evaluated. In all cases, peptides with long acyl chains showed greater LPS-neutralizing activities than the original acetylated peptides. Structural analysis of these peptides revealed that N-acylation with long acyl chains promotes the formation of micellar or fibril-like nanostructures, thus proving a correlation between anti-LPS activity and nanostructure formation. The results of this study provide useful structural insight for the future design of new acyl peptides that strongly bind LPS and therefore act as antisepsis drugs. Furthermore, this nanostructure–biological activity correlation can be translated into other therapeutic areas.

Introduction

Sepsis, including its acute state, septic shock, is the first cause of mortality in intensive care units[1] and is among the leading causes of mortality worldwide. In 2003, septicemia was the 10th foremost cause of death in the US.[2] Sepsis and other infectious diseases are produced by a bacterial endotoxin, the lipopolysaccharide (LPS), a major component of the cell wall in Gram-negative bacteria.[3] LPS recognition by immune system cells is detected on the basis of the pathology.[4] Although low amounts of LPS can be beneficial for the host immune system, continuous exposure to LPS in the mammalian bloodstream induces deregulation of the release of inflammatory cytokines, thereby leading to the pathological condition.[5] The immunogenic cascade is initiated by LPS recognition and binding to the circulating LPS binding protein (LBP), which transfers the bacterial endotoxin to the CD14 receptor.[6,7] This complex binds to the transmembrane receptors of the Toll-Like receptor family (TLR) in order to transduce the signal into the cell, an event that initiates the transcription of cytokine genes.[8]

Research efforts have been directed towards the characterization of the LPS signaling pathway in order to define pharmacological targets.[9–14] However, although inhibitors of tumor necrosis factor (TNF) and other inflammatory mediators have been targeted, this approach has not yet increased the survival rates of septic shock patients.[15,16] There is currently only one USFDA-approved therapy that increases survival in adult patients with high-risk severe sepsis: Xigris (activated drotrecogin alfa), which decreases microvascular dysfunction by reducing inflammation and coagulation, and by increasing fibrinolysis.[17] Although drotrecogin alfa improves survival,[18,19] there are concerns regarding some of the effects of this drug, and complementary agents would improve the therapeutic outcome.[20] In this regard, the inhibition of LPS at the beginning of this process is considered a promising approach. Thus, compounds with the capacity to extracellularly neutralize LPS or its toxic portion, the lipid A moiety, may provide a potential source of useful lead compounds of pharmacological relevance. In this sense, a considerable research effort has been devoted to LPS binding proteins and their derived peptides, as described in a detailed review recently published by Chaby.[21] In the study reported herein, we focused on three LPS binding proteins of distinct origin: 1) the *Limulus* anti-LPS factor (LALF), 2) the bactericidal permeability-increasing protein (BPI), and 3) serum amyloid P (SAP).

LALF is a small (101 amino acids) basic protein that inhibits the LPS-mediated coagulation cascade.[22] An amphipathic loop that spans residues 31–52 has been described as the LPS binding site.[23] Further studies determined the minimal LPS binding domain as a 14-amino acid cyclic peptide named LALF-14c, comprising residues 36–47.[24] Recently, we described an even shorter cyclic peptide, RLKWc, containing key residues Arg41-Leu42-Lys43-Trp44 with activity similar to that of LALF-14c.[25] BPI is a 57-kDa cationic protein from human neutrophils that binds to and neutralizes LPS and has high bactericidal activity against Gram-negative bacteria. It shares a high degree of ho-

[a] C. Mas-Moruno, Dr. L. J. Cruz, Prof. Dr. F. Albericio
Institute for Research in Biomedicine
Barcelona Science Park, 08028 Barcelona (Spain)
Fax: (+34) 93 403 71 26
E-mail: albericio@irbbarcelona.org

[b] C. Mas-Moruno, Dr. L. J. Cruz, Prof. Dr. F. Albericio
CIBER-BBN, Networking Centre on Bioengineering, Biomaterials, and Nanomedicine, 08028 Barcelona (Spain)

[c] L. Cascales, Dr. P. Mora, Prof. Dr. E. Pérez-Payá
Department of Medicinal Chemistry
Centro de Investigación Príncipe Felipe, 46013 Valencia (Spain)

[d] Prof. Dr. E. Pérez-Payá
Instituto de Biomedicina de Valencia
CSIC, 46010 Valencia (Spain)

[e] Prof. Dr. F. Albericio
Department of Organic Chemistry
University of Barcelona, 08028 Barcelona (Spain)

mology with LBP[26] and contains three LPS binding sites (residues 17–45, 65–99, and 142–169).[27] Of these regions, a 15-mer synthetic peptide (residues 85–99) was shown to be bactericidal.[27] Interestingly, the region comprising amino acids 86–104 shows homology with the antiparallel β-sheet folding present in LALF and that participates in LPS binding. The two sequences share a common structural motif, with hydrophobic and cationic β-sheet faces, which facilitates LPS interaction.[28] Finally, SAP is a serum multi-specific glycoprotein that binds LPS and other molecules.[29] SAP has three LPS binding sites (residues 27–39, 61–75, 186–200),[30] but only the latter two are truly accessible for interaction on the protein surface. Moreover, the 15-mer SAP-derived peptide (186–200) protects against LPS-induced septic shock in animal models.[30]

The molecular mechanism by which these proteins neutralize LPS derives from their capacity to recognize and bind the endotoxic lipid A moiety of LPS[33,34] (Figure 1). The requirements to exert effective binding are best described for the cyclic antibiotic peptide polymyxin B (PMB),[35] which contains five positive charges and an N-linked acyl chain. In fact, a C_{12} alkyl acylation of the lactoferrin-derived peptide LF11 results in both changes in its conformational properties, and in an enhancement of its LPS binding affinity.[36–38] Herein, the solid-phase synthesis, structural analysis, and biological activity of N-acylated peptides derived from LALF-14c, BPI, and SAP are described.

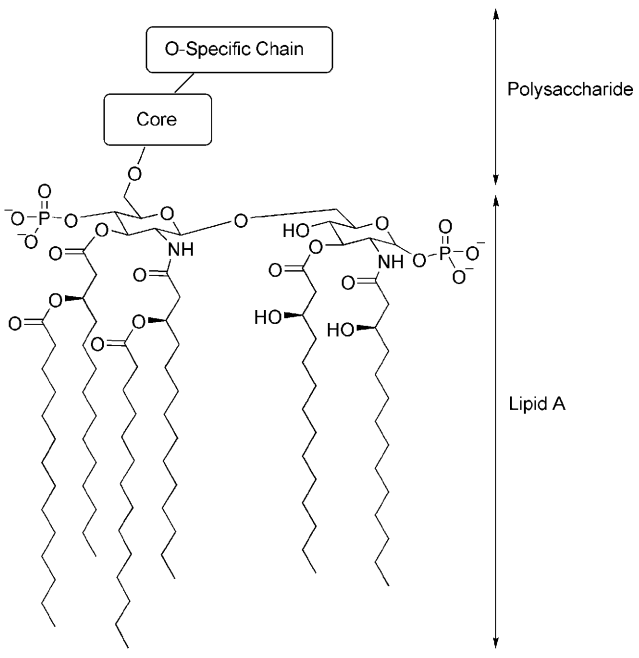

Figure 1. General structure of LPS showing the chemical detail of the lipid A moiety. LPS comprises three covalently linked domains: 1) an O-specific chain, an immunogenic, highly variable repeating polysaccharide that extends into the external medium; 2) an inner core oligosaccharide; and 3) a glycolipid, the so-called lipid A, formed by a 1,4′-bisphosphorylated glucosamine disaccharide that carries several amide- and ester-linked fatty acids.[31,32] The lipid A structure is conserved in all species of Gram-negative bacteria.

Results and Discussion

N-Acylated peptides derived from LALF-14c

The optimal chain length for LPS interaction was studied after conjugation of LALF-14c (H-G[CKPTFRRLKWKYKC]G-NH_2)[1] with distinct aliphatic acids: acetic acid (C_2), butyric acid (C_4), caproic acid (C_6), octanoic acid (C_8), decanoic acid (C_{10}), lauric acid (C_{12}), myristic acid (C_{14}), palmitic acid (C_{16}), stearic acid (C_{18}), and linoleic acid (C_{18} unsaturated). Although the synthesis of acetylated LALF-14c (C_2-LALF-14c) has already been described[39] and can be easily achieved upon cyclization with dimethyl sulfoxide (DMSO), the synthesis of N-acylated derivatives, particularly those with a greater number of carbon units, was more challenging. The solubility of the peptides decreases with increasing chain length. These peptides were prone to aggregation, and were therefore difficult to purify. To overcome this limitation, a new strategy was developed (see Scheme 1): peptides were synthesized on solid phase following an Fmoc/*t*Bu strategy. Cysteine residues were added at the N and C termini to obtain the cyclic peptide that stabilizes the secondary structure.[24] Acyl chains were then introduced onto the free amino group at the N terminus using PyBOP/HOAt/DIEA as coupling reagents. The linear peptides were cleaved from the solid support, purified by semipreparative RP-HPLC (linear peptides at this point do not present solubility problems) and then cycled. When cyclization was completed, the crude products were treated with HP-20 Diaion resin, which, after an easy workup, yielded the cyclic peptides with excellent purities and without further purification. This methodology can be applied to various peptides and is a straightforward procedure to obtain cyclic peptides with low aqueous solubility.

The resulting peptides were characterized by HPLC and mass spectrometry and assayed for anti-LPS activity using the chromogenic *Limulus* amebocyte lysate assay (LAL)[40] (Table 1). C_{18}-LALF-14c and C_{18}-unsat-LALF-14c were discarded for this assay because the former was insoluble in all the aqueous media assayed, and the latter underwent hydration of its saturated bonds under acidic cleavage conditions.

The initial increase in acyl chain length from C_2-LALF-14c to C_4- and C_6-LALF-14c had a minor effect on LPS-neutralizing activity. However, this activity clearly improved for the peptides with longer acyl chains, that is, the C_8-LALF-14c to C_{16}-LALF-14c series. In particular, C_{16}-LALF-14c showed a 10-fold increase in LPS-neutralizing activity over the original C_2-LALF-14c peptide.

Further biological analyses were performed using whole-cell systems. As mentioned above, the pro-inflammatory cytokine TNF is one of the earliest and most important mediators of the LPS-induced immune response.[41] Before testing whether these compounds inhibit the release of TNF in LPS-challenged macrophages, the nonspecific toxicity of the compounds was investigated with MTT assays in RAW 264.7 macrophages. C_{12}-, C_{14}-, and C_{16}-LALF-14c were slightly toxic toward these cells (Figure 2). However, the toxicity profile of C_2-, C_4-, C_6-, C_8-, and

[1] *Brackets [ ] indicate where the peptide is cyclized by a disulfide bridge.*

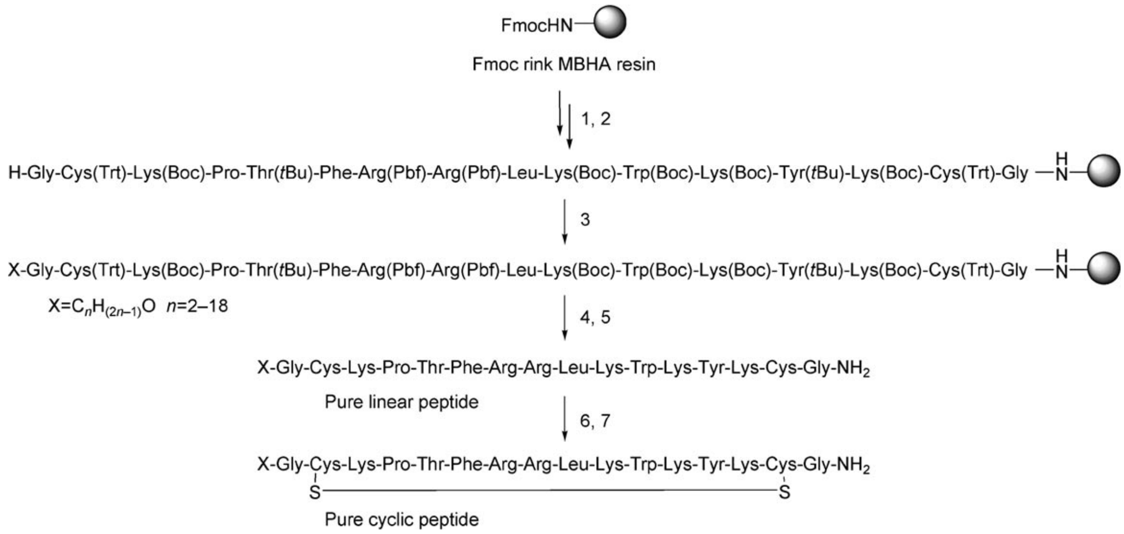

Scheme 1. General procedure for the synthesis of N-acylated LALF-14c-derived peptides: 1) piperidine/DMF (1:4); 2) Fmoc-AA-OH, HOAt, DIC; repeat 15 times; 3) fatty acid, PyBOP, HOAt, DIEA; 4) TFA/H_2O/TIS (95:2.5:2.5); 5) semipreparative HPLC purification; 6) HOAc/DMSO/H_2O (1:3:16), $(NH_4)_2CO_3$; 7) treatment with Diaion HP-20.

C_{10}-LALF-14c could be described as tolerable for this cell system. In fact, C_8- and C_{10}-LALF-14c showed a greater capacity to inhibit LPS-induced TNF production than the parent C_2-LALF-14c peptide (Figure 3). These results, except for those peptides that exceeded the toxicity limits, correlate well with the activities found in the in vitro assay, thereby suggesting that the neutralization of LPS affects cell signaling and could be a valuable approach to control the undesired release of TNF and other cytokines.

Table 1. LPS-neutralizing activity of LALF-14c-derived peptides

Peptide	IC_{50} [μM]	SD
C_2-LALF-14c	37	1.2
C_4-LALF-14c	51	1.1
C_6-LALF-14c	38	1.1
C_8-LALF-14c	15	1.1
C_{10}-LALF-14c	8	1.1
C_{12}-LALF-14c	4	1.1
C_{14}-LALF-14c	3	1.5
C_{16}-LALF-14c	3	1.1

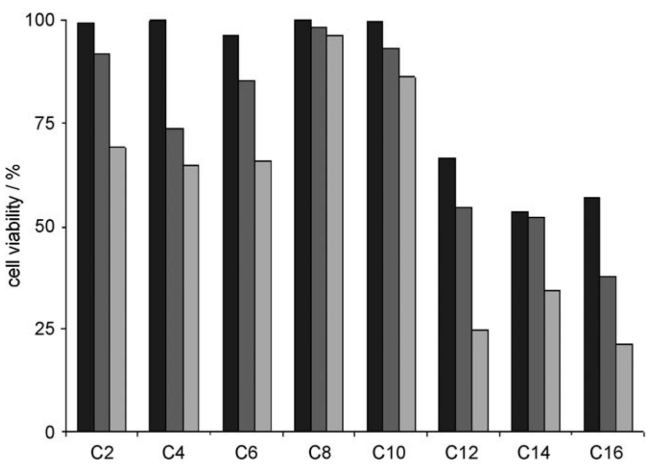

Figure 2. Cell viability is shown at a range of peptide concentrations: 10 (black bars), 5 (gray bars), and 1 μM (light gray bars). Cell viability was evaluated in RAW 264.7 cells by MTT assay, as described in the Experimental Section.

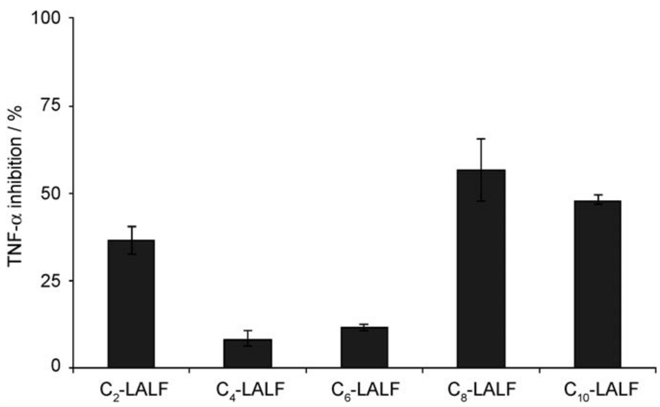

Figure 3. The inhibition of LPS-induced TNF in RAW 264.7 cells is shown. Peptides were tested at a concentration of 10 μM. Only TNF inhibition of nontoxic peptides at this concentration is shown.

Structural studies on LALF-14c-derived peptides

The above results suggested that the acyl moiety plays an important role in the conformation of the peptide, which can affect the biological activity of the peptides. Thus, a comparative analysis of the conformational behavior of C_2- and C_{16}-LALF-14c was carried out by transmission electron microscopy (TEM). The peptides were dissolved in phosphate-buffered saline (PBS) at a concentration range of 0.05–5 $mg\,mL^{-1}$ and stained with 2% uranyl acetate. TEM images (see Figure 4) showed that C_{16}-LALF-14c, but not C_2-LALF-14c, formed

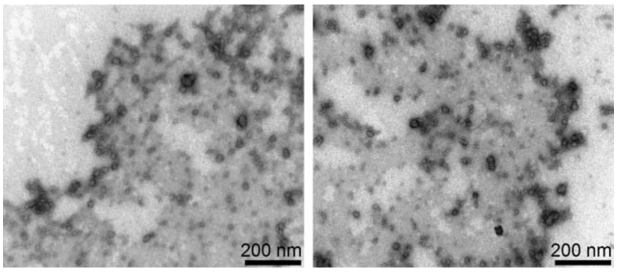

Figure 4. TEM images of C_{16}-LALF-14c. Two representative micrographs are shown. Peptides were dissolved in PBS at 5 mg mL^{-1} and treated as explained in the Experimental Section. All samples were prepared in triplicate, and images obtained were reproducible in all grids.

micelles at 5 mg mL^{-1} (i.e. 2 μM for C_{16}-LALF-14c). This result is consistent with previous studies in which peptide amphiphiles with acyl tails (i.e. C_{16}) are described to form spherical micelles.[42] The diameter of these micelles varied from 15 to 20 nm, and several of these micelles accumulated into aggregates of multiple monomers. Nanoparticle formation strongly depended on peptide concentration. At concentrations <5 mg mL^{-1} the relative abundance of these structures decreased, but they were still observable at 0.05 mg mL^{-1} (images not shown). The extent of these aggregation effects was studied in the rest of the LALF-14c-derived peptides at concentrations of 0.5 mg mL^{-1} in order to determine the minimal acyl chain length required for nanostructure formation. Under assay conditions (see Experimental Section), C_2- and C_4-LALF-14c did not form micelles. C_6- to C_{10}-LALF-14c showed a low tendency to form micelles, but it was not until C_{12}-LALF-14c that the abundance of these aggregates was similar to that observed for C_{16}-LALF-14c (images not shown).

Palmitic acid incorporation in BPI- and SAP-derived peptides

Because C_{16}-LALF-14c presented the highest values of LPS neutralization in the LAL assay and also showed the most dramatic effects in terms of aggregation and nanostructure formation, we were particularly interested in verifying whether this phenomenon could be translated to other anti-LPS peptides such as those derived from BPI and SAP.

Active sequences from BPI (residues 85–100: IKISGKWKAQKRFLKM) and SAP (residues 186–200: QALNYEIRGYVIIKP) were synthesized and N-acetylated or palmitoylated on solid phase. The synthesis of BPI-derived peptides did not represent a challenge. However, SAP contains a hydrophobic sequence (Val-Ile-Ile) and standard solid-phase methods ended with deletion peptides that were very difficult to purify. Microwave (MW)-assisted solid-phase synthesis helped to overcome this problem (see Experimental Section for details). After purification and characterization, the IC_{50} values for these peptides as LPS-neutralizers were calculated using the in vitro assay (Figure 5) and compared against those obtained for LALF-14c analogues.

The acetylated analogues of BPI and SAP, with respective IC_{50} values of 16 ± 7.4 and 8 ± 1.7 μM, were more active than the original C_2-LALF-14c. Nevertheless, the activity of these

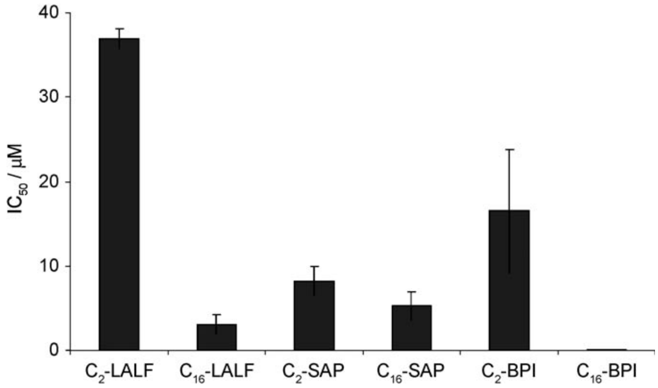

Figure 5. LPS-neutralization activity (IC_{50}) of BPI- and SAP-derived peptides. C_2- and C_{16}-LALF-14c peptides were also included. IC_{50} values are represented as mean values $\pm$SD. The inhibition of the peptides was determined using the chromogenic LAL assay. The assay was performed as described in the Experimental Section.

peptides was again clearly improved with N-terminal palmitoylation. C_{16}-BPI had a greater inhibitory activity (60 nM) than its acetylated analogue, and palmitoylated SAP was almost twofold more active (5.3 ± 1.6 μM) than C_2-SAP. These results are consistent with those obtained for LALF, and highlight the activity enhancement that the fatty acyl chain achieves when it is incorporated to various anti-LPS peptides. The cytotoxicity of these peptides was also evaluated. The results were similar to those obtained for LALF-14c-modified peptides (Figure 6).

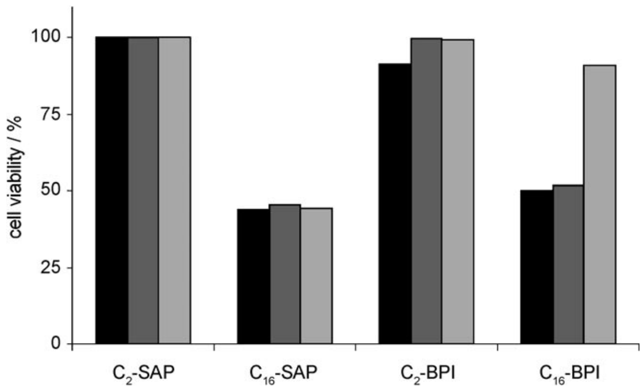

Figure 6. Cytotoxicity of BPI- and SAP-derived peptides. Cell viability is represented at a range of peptide concentrations: 10 (black bars), 5 (gray bars), and 1 μM (light gray bars). Cell viability was evaluated on RAW 264.7 cells by MTT assay as described in the Experimental Section.

Acetylated peptides showed good cell viability, in contrast to palmitoylated derivatives, which displayed some toxicity. C_{16} peptides were hence discarded for TNF inhibition studies in macrophages. However, it is important to note that C_{16}-BPI at 1 μM (concentration above its IC_{50} value) shows low toxicity, and therefore these results demonstrate that promoting the formation of nanostructures on anti-LPS peptides could induce high LPS-neutralizing activity and moderate or total absence of toxicity. The acetylated peptides did not have any relevant activity (data not shown).

The effect of the C_{16} acyl chain on these new peptides was again evaluated by TEM. C_2- and C_{16}-BPI-derived peptides were dissolved in PBS at a concentration of 5 mg mL^{-1}. Alternatively, C_2- and C_{16}-SAP-modified peptides were dissolved in H_2O at 0.5 mg mL^{-1}, because at higher concentrations the palmitoylated derivative was insoluble. Again, no aggregates or defined structures were observed for the acetylated peptides. In contrast, for both C_{16}-BPI and C_{16}-SAP peptides, clear fibril-like nanostructures were detected (Figure 7).

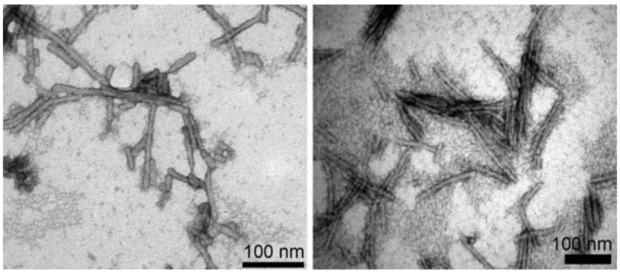

Figure 7. TEM images of C_{16}-BPI and C_{16}-SAP. One representative micrograph is shown for each peptide (C_{16}-BPI: left; C_{16}-SAP: right). C_{16}-BPI was dissolved in PBS at 5 mg mL^{-1}, and C_{16}-SAP was dissolved in H_2O at 0.5 mg mL^{-1}. Peptides were treated as described in the Experimental Section. All samples were prepared in triplicate, and images obtained were reproducible in all grids.

C_{16}-BPI displayed defined tubular structures either alone or associated in multiple fibrils. These fibrils were on average 50–140 nm long and 9–12 nm wide. In contrast, C_{16}-SAP fibrils were more prone to self-associate and aggregate. In this case, fibril length varied from 70 to 130 nm, and width ranged from 10 to 12 nm. These images show the extent of the aggregation properties of these new LALF, BPI, and SAP lipopeptides.

Conclusions

Several N-acylated peptides derived from LALF-14c were synthesized, cyclized, and evaluated for anti-LPS activity. An increase in activity of at least 10-fold was observed for C_{16}-LALF-14c over the parent peptide, C_2-LALF-14c. On the basis of TEM images, these enhanced activities could be associated with the capacity of the peptides to form nanostructures. TEM studies revealed that long fatty acyl chains promote the formation of micellar and fibrilar superstructures. This correlation between biological activity and nanostructure formation has been corroborated with other anti-LPS peptides, BPI, and SAP, which also displayed improved activities. Although some of them show some toxicity in macrophages, these results demonstrate that nanostructure formation can lead to anti-LPS peptides with higher LPS-neutralizing activities at cell-tolerable concentrations. Furthermore, we are currently exploring applications of these peptides at cell-tolerated concentrations as cell-penetrating micellar-based peptides.

Experimental Section

LPS-neutralizing activity: All solutions used in the LPS-neutralizing activity assay were tested to ensure they were endotoxin-free, and material was sterilized by heating for 3 h at 180 °C. LPS from *E. coli* 055:B5 and polymyxin B were purchased from Sigma. LPS-neutralizing activity was measured by using the chromogenic *Limulus* amebocyte lysate (LAL) test[40] following the manufacturer's instructions (Cambrex). LAL reagent contains a clottable protein that is activated in the presence of non-neutralized LPS and is an extremely sensitive indicator of the presence of endotoxin. When activated, this enzyme catalyses the release of *p*-nitroaniline (pNA) from the colorless chromogenic substrate Ac-Ile-Glu-Ala-Arg-pNA. The pNA released was measured photometrically at 405 nm in a Rosys Anthos 2010 microtiter plate reader (Tecnomara AG, Zurich, Switzerland). Peptides were incubated at a range of concentrations (50–0.001 μM) with LPS (100 pg mL^{-1}) in a 96-well microtiter plate for 45 min at 37 °C. Polymyxin B (10 μg mL^{-1}) was used as positive control. LAL (12.5 μL) was added to start the reaction at 37 °C. After 16 min, non-neutralized LPS was detected after 10 min incubation with the chromogenic substrate (25 μL). Acetic acid (25 % *v/v* final concentration) was added to stop the reaction, and the absorbance was monitored at 405 nm in a Multiskan Ascent microtiter plate reader (Thermo Labsystems). IC_{50} values (the concentration necessary to neutralize 50 % of LPS in vitro) were determined by a serial dilution assay using LPS (100 pg mL^{-1}) and a range of peptide concentrations as mentioned above.

Cell culture: Mouse macrophages (RAW 264.7) were obtained from the ATCC (American Type Culture Collection, USA). The cells were grown in Dulbecco's modified Eagle's medium (DMEM, Gibco) supplemented with 10 % fetal bovine serum (FBS, Gibco) and 1 % L-glutamine. The cultures were incubated at 37 °C in a humidified atmosphere of 5 % CO_2, 95 % air. Subcultures of macrophages were prepared every 2–3 days by scraping cells into fresh medium.

MTT cell viability assays: Cell viability was evaluated by means of a 3-(4,5-dimethyl-2-thiazolyl)-2,5-diphenyl-2*H*-tetrazolium bromide (MTT) assay. RAW 264.7 cells were seeded in sterile 96-well microtiter plates at a density of 100 000 cells mL^{-1} in DMEM supplemented with 1 % FBS and allowed to settle for 24 h. Peptides at a range of concentrations were added to the plates, and the cells were further incubated for 24 h. After removal of the medium, the precipitated formazan crystals were dissolved in optical grade DMSO (100 μL), and the plates were read at 570 nm using a Wallac 1420 workstation microtiter plate reader.

Evaluation of TNF expression: RAW 264.7 cells were seeded in 96-well plates at a density of 100 000 cells mL^{-1} in DMEM supplemented with 1 % FBS and allowed to settle for 24 h. Then, LPS (0.5 ng mL^{-1}) was added in the absence or presence of C_x-LALF-14c at a range of concentrations. After 24 h, supernatants were collected and centrifuged for 10 min at 400 *g* and stored at −20 °C until measurement of cytokine content. TNF in the cell supernatant was determined using a commercial ELISA kit (BD Bioscience), following the manufacturer's protocol. Samples were diluted 10-fold with buffer. Color changes at 450 nm were measured using a microtiter plate reader. Cytokine levels were expressed as pg mL^{-1}. The detection range of the ELISA kit was 0–1000 pg mL^{-1}. The TNF content of each sample was assayed three times.

Transmission electron microscopy (TEM): Samples were stained with a conventional negative staining for TEM using 2 % uranyl acetate on Formvar-carbon-coated copper grids. All electron micrographs were obtained with a Jeol JEM 1010 electron microscope (Tokyo, Japan) operating at 80 kV. Images were obtained with a

CCD Megaview III (SIS) camera (Münster, Germany). Three samples were prepared following the procedure, and results obtained by TEM imaging were reproducible.

Chemistry: Rink amide MBHA resin and protected Fmoc-L-amino acids were purchased from Iris Biotech GmbH (Marktredwitz, Germany). Coupling reagents, solvents for peptide synthesis, and other reagents were purchased from commercial suppliers at the highest purity available and used without further purification. Analytical HPLC was performed using a Waters Alliance 2695 chromatography system (Waters, MA, USA) with a PDA 995 detector, a reversed-phase Symmetry C_{18} column (4.6×150 mm, 5 μm), and linear gradients of MeCN with 0.036% trifluoroacetic acid (TFA) into H_2O with 0.045% TFA. The system was run at a flow rate of 1.0 mL min^{-1} over 15 min. Semipreparative HPLC was carried out on a Waters chromatography system with a dual absorbance detector 2487, a reversed-phase Symmetry C_{18} column (30×150 mm, 5 μm) and linear gradients of MeCN with 0.05% TFA into H_2O with 0.1% TFA. The system was run at a flow rate of 20.0 mL min^{-1} over 30 min. HPLC–MS was performed using a Waters Alliance 2796 instrument with a dual absorbance detector 2487 and ESI-MS Micromass ZQ chromatography system (Waters), a reversed-phase Symmetry 300 C_{18} (3.9×150 mm, 5 μm) column, and H_2O with 0.1% formic acid and MeCN with 0.07% formic acid as mobile phases. Mass spectra were recorded on a MALDI Voyager DE RP time-of-flight (TOF) spectrometer (Applied Biosystems, Foster City, CA, USA) using ACH matrix.

All LALF-14c-derived peptides were manually synthesized using the Fmoc/*t*Bu strategy in polypropylene syringes, each fitted with a polyethylene porous disk. Solvents and soluble reagents were removed by suction. Washings between deprotection, couplings, and subsequent deprotection steps were carried out with *N*,*N*-dimethylformamide (DMF) and CH_2Cl_2 using 10 mL solvent per gram of resin each time. The Fmoc group was removed by treatment with piperidine/DMF (1:4 *v*/*v*). Peptide synthesis transformations and washes were performed at 25 °C. BPI was synthesized with an automatic peptide synthesizer ABI 433A (Applied Biosystems) following standard Fmoc chemistry and a FastMoc protocol. SAP was manually synthesized using a Discover SPS Microwave Peptide Synthesizer (CEM Corporation, North Carolina, USA) following the protocols described below.

Synthesis of LALF-14c-derived peptides: Fmoc Rink amide MBHA resin (2.00 g, 0.65 mmol g^{-1}) was placed in a 20-mL polypropylene syringe fitted with a polyethylene filter disk. After Fmoc removal, the coupling reactions were carried out with Fmoc-amino acids (4 equiv), 7-aza-1-hydroxy-1*H*-benzotriazole (HOAt, 4 equiv) and *N*,*N'*-diisopropylcarbodiimide (DIC, 4 equiv) in DMF for 2 h. Couplings were monitored using the Kaiser, de Clercq, or chloranil methods.[43] When necessary, recouplings were done either with *O*-(7-azabenzotriazol-1-yl)-*N*,*N*,*N'*,*N'*-tetramethyluronium hexafluorophosphate (HATU, 4 equiv) and *N*,*N*-diisopropylethylamine (DIEA, 8 equiv) for 30 min, or with 1-benzotriazolyloxytris(pyrrolidino)-phosphonium hexafluorophosphate (PyBOP, 4 equiv), HOAt (4 equiv), and DIEA (12 equiv) for 2 h. After completion of the synthesis, the resin was divided, and acylation treatments were carried out individually. Fatty acids (5 equiv) were coupled using PyBOP (5 equiv), HOAt (5 equiv), and DIEA (15 equiv) for 48 h at room temperature. For C_2-LALF, this protocol was substituted with a standard acetylation step with Ac_2O/DIEA/DMF (10:20:70) for 30 min. For the deprotection of side chain groups and concomitant cleavage of the peptide from the support, the resin was washed with CH_2Cl_2 (3×1 min), dried, and treated with TFA/H_2O/TIS/EDT (95:2:2:1) for 2 h (TIS = triisopropylsilane, EDT = 1,2-ethanedithiol). TFA was then removed by evaporation with nitrogen, and the peptides were precipitated with cold anhydrous *tert*-butylmethyl ether (TBME), dissolved in H_2O/MeCN (distinct mixtures used) and then lyophilized. The linear crude peptides were purified by semipreparative HPLC (see conditions used below). After purification, linear peptides were cycled upon dissolution in a solution of HOAc/DMSO/H_2O (1:3:16) at a concentration of 0.5 mg mL^{-1}. Neutral pH was reached after treatment with ammonium carbonate. The solution was then stirred at room temperature for 24 h and monitored by Ellman's test[44] and/or HPLC. When cyclization was finished, the reaction mixture was treated with the aromatic adsorbent Diaion HP-20 (Supelco, Bellefonte, PA, USA) for 12 h. The peptide adsorbed was gently washed with H_2O to remove all DMSO and was then eluted with increasing concentrations of MeCN in aqueous mixtures. Lyophilization yielded the desired peptides, which were then assayed for biological activity without further purification.

Acetyl-LALF-14c (C_2-LALF-14c): The linear peptide (25.7 mg) was purified by semipreparative HPLC: linear gradient from 10 to 50% MeCN over 30 min, flow rate 20 mL min^{-1}. Obtained: 7.3 mg (purification yield 29%). The purified linear peptide (7.3 mg) was cycled as described above. Obtained: 4.9 mg (cyclization yield 67%). The peptide was characterized by HPLC (10→50% MeCN over 15 min, t_R = 6.44 min, 94%) and MALDI-TOF (*m*/*z* calcd for $C_{92}H_{144}N_{28}O_{19}S_2$: 2009.06, found: 2010.61 $[M+H]^+$, 2033.61 $[M+Na]^+$.

Butyryl-LALF-14c (C_4-LALF-14c): The linear peptide (30.8 mg) was purified by semipreparative HPLC: linear gradient from 10 to 50% MeCN over 30 min, flow rate 20 mL min^{-1}. Obtained: 11.3 mg (purification yield 37%). The purified linear peptide (11.3 mg) was cycled as described above. Obtained: 8.7 mg (cyclization yield 77%). The peptide was characterized by HPLC (10→50% MeCN over 15 min, t_R = 6.83 min, 96%) and MALDI-TOF (*m*/*z* calcd for $C_{94}H_{148}N_{28}O_{19}S_2$: 2037.09, found: 2038.10 $[M+H]^+$, 2060.09 $[M+Na]^+$.

Caproyl-LALF-14c (C_6-LALF-14c): The linear peptide (30.3 mg) was purified by semipreparative HPLC: linear gradient from 20 to 35% MeCN over 30 min, flow rate 20 mL min^{-1}. Obtained: 7.4 mg (purification yield 24%). The purified linear peptide (7.4 mg) was cycled as described above. Obtained: 3.5 mg (cyclization yield 47%). The peptide was characterized by HPLC (0→100% MeCN over 15 min, t_R = 8.39 min, 99%) and MALDI-TOF (*m*/*z* calcd for $C_{96}H_{152}N_{28}O_{19}S_2$: 2065.12, found: 2066.16 $[M+H]^+$, 2088.14 $[M+Na]^+$, 2106.13 $[M+K]^+$.

Octanoyl-LALF-14c (C_8-LALF-14c): The linear peptide (28.7 mg) was purified by semipreparative HPLC: linear gradient from 20 to 35% MeCN over 30 min, flow rate 20 mL min^{-1}. Obtained: 6.2 mg (purification yield 22%). The purified linear peptide (6.2 mg) was cycled as described above. Obtained: 6.2 mg (cyclization yield quant.). The peptide was characterized by HPLC (20→35% MeCN over 15 min, t_R = 5.83 min, 91%) and HPLC–MS (*m*/*z* calcd for $C_{98}H_{156}N_{28}O_{19}S_2$: 2093.15, found: 1046.6 $[M+H]^+/2$, 698.3 $[M+H]^+/3$, 523.7 $[M+H]^+/4$.

Decanoyl-LALF-14c (C_{10}-LALF-14c): The linear peptide (31.5 mg) was purified by semipreparative HPLC: linear gradient from 20 to 35% MeCN over 30 min, flow rate 20 mL min^{-1}. Obtained: 5.1 mg (purification yield 16%). The purified linear peptide (5.1 mg) was cycled as described above. Obtained: 3.6 mg (cyclization yield 71%). The peptide was characterized by HPLC (0→100% MeCN over 15 min, t_R = 7.25 min, 99%) and MALDI-TOF (*m*/*z* calcd for $C_{100}H_{160}N_{28}O_{19}S_2$: 2121.19, found: 2122.44 $[M+H]^+$, 2145.44 $[M+Na]^+$.

Lauryl-LALF-14c (C_{12}-LALF-14c): The linear peptide (40.2 mg) was purified by semipreparative HPLC: linear gradient from 20 to 40% MeCN over 30 min, flow rate 20 mL min^{-1}. Obtained: 7.7 mg (purification yield 19%). The purified linear peptide (7.7 mg) was cycled as described above. Obtained: 5.5 mg (cyclization yield 71%). The peptide was characterized by HPLC (0→100% MeCN over 15 min, t_R=7.69 min, 99%) and MALDI-TOF (*m/z* calcd for $C_{102}H_{164}N_{28}O_{19}S_2$: 2149.22, found: 2150.43 $[M+H]^+$, 2173.43 $[M+Na]^+$, 2188.44 $[M+K]^+$.

Myristyl-LALF-14c (C_{14}-LALF-14c): The linear peptide (32.8 mg) was purified by semipreparative HPLC: linear gradient from 30 to 40% MeCN over 30 min, flow rate 20 mL min^{-1}. Obtained: 5.7 mg (purification yield 17%). The purified linear peptide (5.7 mg) was cycled as described above. Obtained: 3.2 mg (cyclization yield 56%). The peptide was characterized by HPLC (0→100% MeCN over 15 min, t_R=8.17 min, 88%) and MALDI-TOF (*m/z* calcd for $C_{102}H_{164}N_{28}O_{19}S_2$: 2177.25, found: 2178.47 $[M+H]^+$, 2200.44 $[M+Na]^+$, 2216.44 $[M+K]^+$.

Palmitoyl-LALF-14c (C_{16}-LALF-14c): The linear peptide (33.3 mg) was purified by semipreparative HPLC: linear gradient from 35 to 45% MeCN over 30 min, flow rate 20 mL min^{-1}. Obtained: 9.0 mg (purification yield 27%). The purified linear peptide (9.0 mg) was cycled as described above. Obtained: 5.6 mg (cyclization yield 62%). The peptide was characterized by MALDI-TOF (*m/z* calcd for $C_{106}H_{172}N_{28}O_{19}S_2$: 2205.28, found: 2205.83 $[M+H]^+$, 2227.82 $[M+Na]^+$, 2245.80 $[M+K]^+$.[2]

Synthesis of BPI-derived peptides: The automatic synthesis was conducted on Fmoc Rink amide MBHA resin (154 mg, 0.65 mmol g^{-1}) on a 0.1-mmol scale with a 10-fold excess of Fmoc-protected L-amino acids and *O*-benzotriazol-1-yl-*N*-tetramethyluronium tetrafluoroborate (TBTU, 0.45 M) in the presence of 1-hydroxy-1*H*-benzotriazole (HOBt) in DMF as coupling reagents. The synthesis was carried out with deprotection and coupling steps of 15 and 35 min, respectively. After the assembly was completed, the peptide resin was washed with CH_2Cl_2 and divided in two. The peptide was acetylated or palmitoylated as indicated above. Cleavage of each fraction and subsequent workup was done as explained before. The linear peptides were purified and characterized as follows.

Acetyl-BPI (C_2-BPI): The peptide (18.3 mg) was purified by semipreparative HPLC: linear gradient from 5 to 60% MeCN over 30 min, flow rate 20 mL min^{-1}. Obtained: 10.4 mg (purification yield 57%). The peptide was characterized by HPLC (0→100% MeCN over 15 min, t_R=6.38 min, 99%) and HPLC–MS (*m/z* calcd for $C_{94}H_{159}N_{27}O_{19}S$: 2002.20, found: 1001.9 $[M+H]^+/2$, 668.2 $[M+H]^+/3$, 501.5 $[M+H]^+/4$.

Palmitoyl-BPI (C_{16}-BPI): The peptide (21.3 mg) was purified by semipreparative HPLC: linear gradient from 20 to 100% MeCN over 30 min, flow rate 20 mL min^{-1}. Obtained: 11.9 mg (purification yield 56%). The peptide was characterized by HPLC (0→100% MeCN over 15 min, t_R=9.17 min, 98%) and HPLC–MS (*m/z* calcd for $C_{108}H_{187}N_{27}O_{19}S$: 2198.42, found: 1100.0 $[M+H]^+/2$, 733.6 $[M+H]^+/3$, 550.5 $[M+H]^+/4$.

Synthesis of SAP-derived peptides: The synthesis was performed on Fmoc Rink amide MBHA resin (400 mg, 0.70 mmol g^{-1}) using MW conditions. Couplings were carried out with Fmoc-protected L-amino acids (4 equiv), HOAt (4 equiv), and DIC (4 equiv) in DMF for 10 min at 75 °C (MW, 20 W). Recouplings were done by repeating the same conditions or with HATU (4 equiv) and DIEA (8 equiv) in DMF for 10 min at 75 °C (MW, 20 W). The Fmoc group was removed by treatment with piperidine/DMF (1:4 *v/v*) for 5 min at 75 °C (MW, 20 W). After the assembly was completed, the peptide resin was washed with CH_2Cl_2, divided in two, and treated as explained above for BPI.

Acetyl-SAP (C_2-SAP): The peptide (36.8 mg) was purified by semipreparative HPLC: linear gradient from 5 to 95% MeCN over 30 min, flow rate 20 mL min^{-1}. Obtained: 4.2 mg (purification yield 11%). The peptide was characterized by HPLC (5→100% MeCN over 15 min, t_R=6.74 min, 82%) and MALDI-TOF (*m/z* calcd for $C_{85}H_{136}N_{22}O_{22}$: 1817.02, found: 1818.31 $[M+H]^+$, 1840.31 $[M+Na]^+$, 1856.29 $[M+K]^+$.

Palmitoyl-SAP (C_{16}-SAP): The peptide (19.0 mg) was purified by semipreparative HPLC: linear gradient from 30 to 80% MeCN over 30 min, flow rate 20 mL min^{-1}. Obtained: 1.8 mg (purification yield 10%). The peptide was characterized by HPLC (30→100% MeCN over 15 min, t_R=7.79 min, 86%) and MALDI-TOF (*m/z* calcd for $C_{99}H_{164}N_{22}O_{22}$: 2013.24, found: 2014.33 $[M+H]^+$, 2036.32 $[M+Na]^+$, 2052.29 $[M+K]^+$.

[2] *In this case, characterization by HPLC was not possible due to the presence of aggregates in the chromatogram profile. After a reducing treatment, these aggregates disappear, and a single reduced peak is obtained, which implies good final purity.*

Acknowledgements

The authors thank Dr. Mateu Pla and Elisenda Coll for their kind help with the TEM images. This work was partially supported by Fundació La Marató de TV3, CICYT (BIO2004-998 and CTQ2006-03794/BQU), Instituto de Salud Carlos III (CB06_01_0074), the Generalitat de Catalunya (2005SGR 00662), Centro de Investigación Príncipe Felipe, the Institute for Research in Biomedicine, and the Barcelona Science Park.

Keywords: biological activity · drug design · lipopeptides · medicinal chemistry · structure–activity relationships

[1] M. H. Silverman, M. J. Ostro, *Bacterial Endotoxin in Human Disease: How Advances in Understanding the Role of Gram-Negative Bacteria and Endotoxin in Infectious Diseases and Complications May Improve the Development of Diagnostic and Treatment Options* **1998**, Xoma Ltd., Berkeley, CA, USA. http://xomaprdev.zoomedia.com/pdfs/kpmgendo.pdf (last accessed September 23, 2008).
[2] M. P. Heron, B. L. Smith, *Natl. Vital Stat. Rep.* **2007**, *55*, 1–93.
[3] E. T. Rietschel, H. Brade, O. Holst, L. Brade, S. Muller-Loennies, U. Mamat, U. Zahringer, F. Beckmann, U. Seydel, K. Brandenburg, A. J. Ulmer, T. Mattern, H. Heine, J. Schletter, H. Loppnow, U Schonbeck, H. D. Flad, S. Hauschildt, U. Schade, F. Di Padova, S. Kusumoto, R. R. Schumann, *Curr. Top. Microbiol. Immunol.* **1996**, *216*, 39–81.
[4] N. C. Riedemann, R. F. Guo, P. A. Ward, *Nat. Med.* **2003**, *9*, 517–524.
[5] R. L. Modlin, H. D. Brightbill, P. J. Godowski, *N. Engl. J. Med.* **1999**, *340*, 1834–1835.
[6] E. Hailman, H. S. Lichenstein, M. M. Wurfel, D. S. Miller, D. A. Johnson, M. Kelley, L. A. Busse, M. M. Zukowski, S. D. Wright, *J. Exp. Med.* **1994**, *179*, 269–277.
[7] R. R. Schumann, E. T. Rietschel, H. Loppnow, *Med. Microbiol. Immunol.* **1994**, *183*, 270–297.
[8] K. V. Anderson, *Curr. Opin. Immunol.* **2000**, *12*, 13–19.
[9] X. Sáez-Llorens, G. H. McCracken, Jr., *J. Pediatr.* **1993**, *123*, 497–508.
[10] J. B. Parent, H. Gazzano-Santoro, D. M. Wood, E. Lim, P. T. Pruyne, P. W. Trown, P. J. Conlon, *Circ. Shock* **1992**, *38*, 63–73.
[11] R. C. Bone, *Crit. Care Med.* **1995**, *23*, 1313–1315.

[12] C. J. Fischer, J. Zimmerman, M. B. Khazaeli, T. E. Albertson, R. P. Dellinger, E. A. Panacek, G. E. Foulke, C. Dating, C. R. Smith, A. F. LoBuglio, *Crit. Care Med.* **1990**, *18*, 1311–1315.
[13] E. J. Ziegler, *N. Engl. J. Med.* **1991**, *324*, 429–436.
[14] L. Shapiro, J. A. Gelfand, *New Horiz.* **1993**, *1*, 13–22.
[15] C. J. Fisher, G. J. Slotman, S. M. Opal, J. P. Pribble, R. C. Bone, Emmanuel, D. Ng, D. C. Bloedow, M. A. Catalano, *Crit. Care Med.* **1994**, *21*, 12–21.
[16] E. Abraham, A. Anzueto, G. Gutierrez, S. Tessler, G. San Pedro, R. Wunderink, A. Dal Nogare, S. Nasraway, S. Berman, R. Cooney, H. Levy, R. Baughman, M. Rumbak, R. B. Light, L. Poole, R. Allred, J. Constant, J. Pennington, S. Porter, *Lancet* **1998**, *351*, 929–933.
[17] USFDA Application No. (BLA) 125029, source: http://www.fda.gov/cder/index.html.
[18] G. R. Bernard, J. L. Vincent, P. F. Laterre, S. P. LaRosa, J. F. Dhainaut, A. Lopez-Rodriguez, J. S. Steingrub, G. E. Garber, J. D. Helterbrand, E. W. Ely, C. J. Fisher, *N. Engl. J. Med.* **2001**, *344*, 699–709.
[19] P. F. Laterre, D. R. Nelson, W. Macias, E. Abraham, A. Sashegyi, M. D. Williams, M. Levy, B. Utterback, J. L. Vincent, *J. Crit. Care* **2007**, *22*, 142–152.
[20] V. Costa, J. M. Brophy, *BMC Anesthesiol.* **2007**, *7*, 5.
[21] R. Chaby, *Cell. Mol. Life Sci.* **2004**, *61*, 1697–1713.
[22] J. Aketagawa, T. Miyata, S. Ohtsubo, T. Nakamura, T. Morita, H. Hayashida, T. Miyata, S. Iwanaga, T. Takao, Y. Shimonishi, *J. Biol. Chem.* **1986**, *261*, 7357–7365.
[23] A. Hoess, S. Watson, G. R. Siber, R. Liddington, *EMBO J.* **1993**, *12*, 3351–3356.
[24] C. Ried, C. Wahl, T. Miethke, G. Wellnhofer, C. Landgraft, J. Schneider-Mergener, A. Hoess, *J. Biol. Chem.* **1996**, *271*, 28 120–28 127.
[25] P. Mora, C. Mas-Moruno, S. Tamborero, L. J. Cruz, E. Pérez-Payá, F. Albericio, *J. Pept. Sci.* **2006**, *12*, 491–496.
[26] L. J. Beamer, S. F. Carroll, D. Eisenberg, *Protein Sci.* **1998**, *7*, 906–914.
[27] R. G. Little, D. N. Kelner, E. Lim, D. J. Burke, P. J. Conlon, *J. Biol. Chem.* **1994**, *269*, 1865–1872.
[28] B. H. Gray, J. R. Haseman, K. H. Mayo, *Biochim. Biophys. Acta Gen. Subj.* **1995**, *1244*, 185–190.
[29] R. W. Loveless, G. Floyd-O'Sullivan, J. G. Raynes, C. T. Yuen, T. Feizi, *EMBO J.* **1992**, *11*, 813–819.
[30] C. J. de Haas, R. van der Zee, B. Benaissa-Trouw, K. P. van Kessel, J. Verhoef, J. A. van Strijp, *Infect. Immun.* **1999**, *67*, 2790–2796.
[31] E. T. Rietschel, H. Brade, L. Brade, W. Kaca, K. Kawahara, B. Lindner, T. Luederitz, T. Tomita, U. Schade, et al., *Prog. Clin. Biol. Res.* **1985**, *189*, 31–51.
[32] M. Imoto, S. Kusumoto, T. Shiba, E. T. Rietschel, C. Galanos, O. Luederitz, *Tetrahedron Lett.* **1985**, *26*, 907–908.
[33] U. Seydel, A. B. Schromm, R. Blunck, K. Brandenburg, *Chem. Immunol.* **2000**, *74*, 5–24.
[34] K. Brandenburg, U. Seydel, A. B. Schromm, H. Loppnow, M. H. Koch, E. T. Rietschel, *J. Endotoxin Res.* **1996**, *3*, 173–178.
[35] H. Tsubery, I. Ofek, S. Cohen, M. Fridkin, *J. Med. Chem.* **2000**, *43*, 3085–3092.
[36] J. Andrae, K. Lohner, S. E. Blondelle, R. Jerala, I. Moriyon, M. H. J. Koch, P. Garidel, K. Brandenburg, *Biochem. J.* **2005**, *385*, 135–143.
[37] A. Majerle, J. Kidric, R. Jerala, *J. Antimicrob. Chemother.* **2003**, *51*, 1159–1165.
[38] B. Japelj, M. Zorko, A. Majerle, P. Pristovsek, S. Sanchez-Gomez, G. Martinez de Tejada, I. Moriyon, S. E. Blondelle, K. Brandenburg, J. Andrae, K. Lohner, R. Jerala, *J. Am. Chem. Soc.* **2007**, *129*, 1022–1023.
[39] J. P. Tam, C. R. Wu, W. Liu, J. W. Zhang, *J. Am. Chem. Soc.* **1991**, *113*, 6657–6662.
[40] *Guideline on validation of the limulus amebocyte lysate test as an end-product endotoxin test for human and animal parental drugs, biological products and medical services*, US Department of Health and Human Services, P.H.S., US Food and Drug Administration, **1987**.
[41] C. Alexander, E. T. Rietschel, *J. Endotoxin Res.* **2001**, *7*, 167–202.
[42] T. Gore, Y. Dori, Y. Talmon, M. Tirrell, H. Bianco-Peled, *Langmuir* **2001**, *17*, 5352–5360.
[43] J. Vazquez, G. Qushair, F. Albericio, *Methods Enzymol.* **2003**, *369*, 21–35.
[44] G. L. Ellman, *Arch. Biochem. Biophys.* **1959**, *82*, 70–77.

Received: July 4, 2008
Revised: July 25, 2008
Published online on October 2, 2008

